

Original citation:

LHCb Collaboration (Including: Back, J. J., Craik, D., Dossett, D., Gershon, Timothy J., Harrison, P. F., Kreps, Michal, Latham, Thomas, Pilar, T., Poluektov, Anton, Reid, M. M., Silva Coutinho, R., Whitehead, M. and Williams, M. P.) (2012) Measurement of the effective $B_0 \rightarrow K+K^-$ lifetime. Physics Letters B, Volume 716 (Number 3-5). pp. 393-400.

Permanent WRAP url:

<http://wrap.warwick.ac.uk/50353>

Copyright and reuse:

The Warwick Research Archive Portal (WRAP) makes this work of researchers of the University of Warwick available open access under the following conditions.

This article is made available under the Creative Commons Attribution- 3.0 Unported (CC BY 3.0) license and may be reused according to the conditions of the license. For more details see <http://creativecommons.org/licenses/by/3.0/>

A note on versions:

The version presented in WRAP is the published version, or, version of record, and may be cited as it appears here.

For more information, please contact the WRAP Team at: publications@warwick.ac.uk

warwick**publications**wrap

highlight your research

<http://wrap.warwick.ac.uk/>



Measurement of the effective $B_s^0 \rightarrow K^+K^-$ lifetime [☆]

LHCb Collaboration

ARTICLE INFO

Article history:

Received 25 July 2012

Received in revised form 15 August 2012

Accepted 19 August 2012

Available online 21 August 2012

Editor: L. Rolandi

Keywords:

Flavour physics

Lifetime

B physics

ABSTRACT

A precise determination of the effective $B_s^0 \rightarrow K^+K^-$ lifetime can be used to constrain contributions from physics beyond the Standard Model in the B_s^0 meson system. Conventional approaches select B meson decay products that are significantly displaced from the B meson production vertex. As a consequence, B mesons with low decay times are suppressed, introducing a bias to the decay time spectrum which must be corrected. This analysis uses a technique that explicitly avoids a lifetime bias by using a neural network based trigger and event selection. Using 1.0 fb^{-1} of data recorded by the LHCb experiment, the effective $B_s^0 \rightarrow K^+K^-$ lifetime is measured as 1.455 ± 0.046 (stat.) ± 0.006 (syst.) ps.

© 2012 CERN. Published by Elsevier B.V. All rights reserved.

1. Introduction

The study of charmless b -hadron decays can be used to explore the phase structure of the CKM matrix and to search for indirect evidence of physics beyond the Standard Model (SM). A measurement of the effective lifetime of the $B_s^0 \rightarrow K^+K^-$ decay (charge conjugate modes are implied throughout) is of considerable interest as it is sensitive to new physical phenomena affecting the B_s^0 mixing phase and entering the decay at loop level [1–4].

The $B_s^0 \rightarrow K^+K^-$ decay was first observed by the CDF Collaboration [5] and the most precise measurement to date of the effective lifetime was made by the LHCb Collaboration using data taken during 2010 [6]. A detailed theoretical description of the $B_s^0 \rightarrow K^+K^-$ decay can be found in Refs. [3,4]. When the initial flavour of the B_s^0 meson is unknown the decay time distribution can be written as

$$\Gamma(t) \propto (1 - \mathcal{A}_{\Delta\Gamma_s})e^{-\Gamma_L t} + (1 + \mathcal{A}_{\Delta\Gamma_s})e^{-\Gamma_H t}. \quad (1)$$

The quantities Γ_H and Γ_L are the decay widths of the heavy and light B_s^0 mass eigenstates and $\Delta\Gamma_s = \Gamma_L - \Gamma_H$ is the decay width difference. The parameter $\mathcal{A}_{\Delta\Gamma_s}$ is defined as $\mathcal{A}_{\Delta\Gamma_s} = -2\text{Re}(\lambda)/(1 + |\lambda|^2)$ where $\lambda = (q/p)(\bar{A}/A)$, where the complex coefficients p and q define the mass eigenstates of the B_s^0 - \bar{B}_s^0 system in terms of the flavour eigenstates (see e.g., Ref. [7]) and A (\bar{A}) is the amplitude for a B_s^0 (\bar{B}_s^0) meson to decay to the K^+K^- final state.

If the decay time distribution given by Eq. (1) is fitted with a single exponential function the *effective lifetime* is given by [8]

$$\begin{aligned} \tau_{KK} &= \frac{\tau_{B_s^0}}{1 - y_s^2} \left[\frac{1 + 2\mathcal{A}_{\Delta\Gamma_s} y_s + y_s^2}{1 + \mathcal{A}_{\Delta\Gamma_s} y_s} \right] \\ &= \tau_{B_s^0} (1 + \mathcal{A}_{\Delta\Gamma_s} y_s + \mathcal{O}(y_s^2)), \end{aligned} \quad (2)$$

where $\tau_{B_s^0} = 2/(\Gamma_H + \Gamma_L) = \Gamma_s^{-1}$ and $y_s = \Delta\Gamma_s/2\Gamma_s$. The K^+K^- final state is CP -even and so in the SM the decay is dominated by the light mass eigenstate such that $\mathcal{A}_{\Delta\Gamma_s} = -0.972 \pm 0.012$ [3, 9] and the effective lifetime thus is approximately equal to Γ_L^{-1} . Adopting the approach of Ref. [3] and using the world averages of Γ_s and $\Delta\Gamma_s$ [10] and the SM prediction of $\mathcal{A}_{\Delta\Gamma_s}$, the effective lifetime is predicted to be $\tau_{KK} = 1.40 \pm 0.02$ ps. However, the $B_s^0 \rightarrow K^+K^-$ decay is dominated by penguin diagrams and so is sensitive to physics beyond the SM entering at loop level, which may affect $\mathcal{A}_{\Delta\Gamma_s}$. The measurement is also sensitive to new physics contributions to the B_s^0 mixing phase which in turn affects $\Delta\Gamma_s$ [11]. Deviations from this prediction will therefore provide evidence of new physics.

Conventional selections exploit the long lifetimes of b -hadrons by requiring that their decay products are significantly displaced from the primary interaction point. However, this introduces a time-dependent acceptance of the selected b -hadron candidates which needs to be taken into account in the analysis. This Letter describes a technique based on neural networks which avoids such acceptance effects. Only properties independent of the decay time are used to discriminate between signal and background. To exploit the available information, including the correlations between

[☆] © CERN for the benefit of the LHCb Collaboration.

variables, several neural networks are used in a dedicated trigger and event selection.

2. The LHCb experiment and simulation software

The $B_s^0 \rightarrow K^+K^-$ lifetime is measured using 1.0 fb^{-1} of pp collision data collected by the LHCb detector at a centre of mass energy of $\sqrt{s} = 7 \text{ TeV}$ during 2011. The LHCb detector [12] is a single arm spectrometer with a pseudorapidity acceptance of $2 < \eta < 5$ for charged particles. The detector includes a high precision tracking system, which consists of a silicon vertex detector and dedicated tracking planes. The tracking planes consist of silicon microstrip detectors in the region with high charged-particle flux close to the beam pipe and straw tube detectors which provide coverage up to the edge of the LHCb geometrical acceptance. The tracking planes are located either side of the dipole magnet to allow the measurement of the momenta of charged particles as they traverse the detector. Excellent particle identification capabilities are provided by two ring imaging Cherenkov detectors which allow charged pions, kaons and protons to be distinguished from each other in the momentum range 2–100 GeV/c. The energy of particles traversing the detector is measured using a calorimeter system which is sensitive to photons and electrons, as well as hadrons. Muons are identified using a dedicated detector system.

The experiment employs a multi-level trigger comprised of a hardware trigger which uses information from the calorimeter and muon system and a software trigger which performs a full reconstruction of the event, including tracks and vertices.

The simulated events used in this analysis are produced using the PYTHIA 6.4 generator [13], with a choice of parameters specifically configured for LHCb [14]. The EVTGEN package [15] describes the decay of b -hadrons and the GEANT4 toolkit [16] simulates the detector response, implemented as described in Ref. [17]. QED radiative corrections to the $B_s^0 \rightarrow K^+K^-$ decay are generated with the PHOTOS package [18].

3. Trigger and event selection

At LHCb, b -hadrons are produced with an average momentum of around 100 GeV/c and have decay vertices displaced from the primary interaction vertex. Combinatorial background candidates, produced by the random combination of tracks, tend to have low momentum and originate from a primary pp collision vertex. These features are typically exploited to select b -hadrons and reject background. The distance of closest approach (impact parameter) of b -hadron decay products to any primary vertex is a particularly important discriminant in the trigger because it is an order of magnitude faster to compute than the momenta of the same decay products. For this reason, the majority of triggers for hadronic b -hadron decays begin by selecting tracks with a significant displacement from any primary vertex. However, such requirements introduce a time-dependent acceptance which biases the decay time distribution of the selected b -hadron candidates and a significant investment of effort is often required to correct for this bias.

The analysis presented here uses an approach that selects b -hadrons without biasing the decay time distribution, other than trivially through a simple minimum decay time requirement, limiting the systematic uncertainties associated with correcting for any time-dependent acceptance effects. This is achieved using neural networks based on the NeuroBayes package [19] in the software trigger and event selection. Neural networks have advantages over traditional “cut-based” approaches since they are able to exploit the correlations between variables in order to increase signal purity, allowing b -hadrons to be selected without resorting to requirements on impact parameters or flight distance.

The LHCb software trigger has two stages which run sequentially. Due to restrictions on processing time it is not possible to employ a neural network in the first level of the software trigger. Instead, only tracks that are not used in the first level decision are passed to the second trigger level in order to avoid a potential bias. These tracks are required to pass a loose pre-selection with requirements on their momenta, transverse momenta and track fit quality. The tracks are then combined to form B meson candidates, using a kaon mass hypothesis for both tracks, and further requirements are made on the distance of closest approach of the two tracks to each other, the mass of the resulting candidate, the helicity angle of the tracks in the B meson rest frame and the quality of the decay vertex fit.

After this pre-selection the candidates pass through a first neural network, trained on simulated $B_s^0 \rightarrow K^+K^-$, $B^0 \rightarrow K^+\pi^-$ and background events, which uses the momenta and transverse momenta of the tracks and B meson candidate, the distance of closest approach of the two tracks, helicity angle, the χ^2 of the vertex fit and the uncertainty on the fitted B meson mass to discriminate between signal and background. After this stage the data rate is reduced to a level such that each event may be fully reconstructed, including information from the particle identification system. A second network, trained on the same simulated events, uses the information presented to the first network along with particle identification information to further increase the purity of B mesons in the selected candidates.

Roughly half way through 2011 the luminosity delivered by the LHC accelerator increased to a level such that it was necessary to require that the decay time of B meson candidates exceeded 0.3 ps in order to keep the trigger rate within acceptable limits. This requirement only biases the decay time distribution in a trivial way, except through a possible difference in the decay time resolutions of the trigger and offline reconstruction software.

After the trigger, the tracks associated to the selected candidates are removed from the primary vertex fit to avoid a potential bias in the measured decay time. The purity of signal candidates is then further enhanced using two additional sequential neural networks. The first network is trained using simulated events and combines the same information used by the trigger networks along with particle identification information, the energy of each track from the calorimeter, the probability that either track is formed from the association of random hits in the detector and the χ^2 per degree of freedom for both track fits. This network benefits from the more detailed full event reconstruction which is not available in the trigger.

The second network is trained on the data recorded in 2011 using $sWeights$ [20], which are calculated in a window around the signal peak and in the upper sideband region ($5.45 < m_{K^+K^-} < 5.85 \text{ GeV}/c^2$) of the invariant mass spectrum. The $sWeights$ are obtained from a fit to the invariant mass spectrum of the candidates and the neural network uses them to discriminate between signal and background. This network uses the output of the first network as input, all the input variables used by the first network, the uncertainty on the decay time of the B meson candidate and the impact parameter of the B meson candidate with respect to the primary interaction vertex. Only candidates with a decay time of $\tau > 0.3 \text{ ps}$ are used in the network training.

The event selection is determined by making a requirement on the output of this second neural network that maximises the metric $s/\sqrt{s+b}$, where s is the number of signal decays in the region $5.05 < m_{K^+K^-} < 5.85 \text{ GeV}/c^2$ and b is the number of background combinations.

The trigger and offline software reconstruct B meson decay times with different resolutions. Potential “edge-effects” introduced by the trigger requirement that $\tau > 0.3 \text{ ps}$ are avoided by

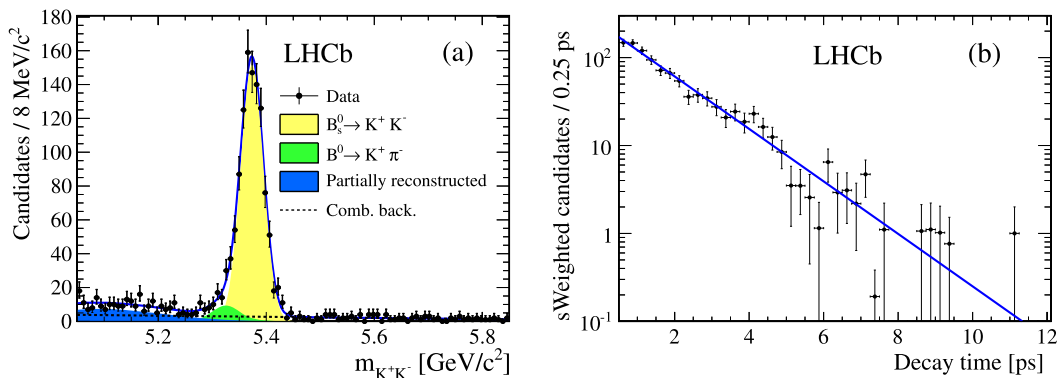


Fig. 1. (a) Invariant mass spectrum for all selected $B_s^0 \rightarrow K^+K^-$ candidates. (b) Decay time distribution of $B_s^0 \rightarrow K^+K^-$ signal extracted using *sWeights* and the fitted exponential function.

requiring that candidates satisfy $\tau > 0.5$ ps in the final event selection. The contribution from the $B^0 \rightarrow K^+\pi^-$ and $B_s^0 \rightarrow K^+K^-$ modes are separated by demanding tight requirements on the particle identification properties of the final state particles. A small level of contamination from decays of Λ_b baryons is further suppressed by demanding that the final state particles are not compatible with the proton hypothesis.

4. Analysis of the effective $B_s^0 \rightarrow K^+K^-$ lifetime

The effective $B_s^0 \rightarrow K^+K^-$ lifetime is evaluated using an unbinned log-likelihood fit. A fit to the invariant mass spectrum is performed to determine the *sWeights* that are used to isolate the $B_s^0 \rightarrow K^+K^-$ decay time distribution from the residual background. The $B_s^0 \rightarrow K^+K^-$ signal component is described by a Gaussian function. The background contamination from partially reconstructed B meson decays is described by a further Gaussian function and the combinatorial background is described by a Chebychev polynomial with one free parameter. It should be noted that the kaon mass is assigned to both final state particles in the vertex fit and hence the reconstructed $B^0 \rightarrow K^+\pi^-$ mass is shifted towards higher values than the nominal mass, creating an asymmetric distribution. The $B^0 \rightarrow K^+\pi^-$ signal component is therefore described by a Crystal Ball function [21] with the tail on high mass side. The parameters of this distribution are fixed using a fit to the independent $B^0 \rightarrow K^+\pi^-$ sample, separated using particle identification information.

The fit finds 997 ± 34 $B_s^0 \rightarrow K^+K^-$ decays and 78 ± 17 $B^0 \rightarrow K^+\pi^-$ decays in the data with 253 ± 25 and 169 ± 20 combinatorial background and partially reconstructed combinations respectively. Fig. 1(a) shows the resulting invariant mass spectrum for $B_s^0 \rightarrow K^+K^-$ candidates.

Using the *sWeights* returned by the mass fit, the $B_s^0 \rightarrow K^+K^-$ decay time distribution is extracted from data using the *sPlot* technique [20]. Since there is no acceptance bias to correct for, the lifetime is determined using a fit of the convolution of an exponential and Gaussian function to account for the resolution of the detector. The mean of the Gaussian function is fixed to zero and its width is fixed to the expected resolution from simulated events, which is $\sigma_t = 0.04$ ps.

The effective $B_s^0 \rightarrow K^+K^-$ lifetime is found to be

$$\tau_{KK} = 1.455 \pm 0.046 \text{ (stat.) ps.}$$

Fig. 1(b) shows the corresponding fit to the decay time distribution of $B_s^0 \rightarrow K^+K^-$ signal.

Since the decay $B^0 \rightarrow K^+\pi^-$ has similar kinematics, it can be used as a control mode. However, since the kaon mass hypothesis is assigned to both tracks, the measured decay time is biased to

Table 1

Contributions to the systematic uncertainty on the effective $B_s^0 \rightarrow K^+K^-$ lifetime measurement. The total uncertainty is calculated by adding the individual contributions in quadrature.

Systematic sources	Uncertainty on τ_{KK} [fs]
Reconstruction efficiency	5
Signal model	1
Background model	1
Length scale	1
Minimum decay time requirement	1
Production asymmetry	2
Total	6

larger values for $B^0 \rightarrow K^+\pi^-$. To avoid this bias a fit is made to the reduced decay time, which is defined as the decay time divided by the invariant mass. This quantity is independent of the mass assigned to the two tracks and is also unbiased by the selection, following an exponential distribution with decay constant equal to m_{B^0}/τ_{B^0} .

Using the value of the B^0 mass [7] as input, the B^0 lifetime is found to be

$$\tau_{B^0} = 1.536 \pm 0.031 \text{ (stat.) ps}$$

which agrees with the current world-average $\tau_{B^0} = 1.519 \pm 0.007$ ps [7].

5. Evaluation of systematic uncertainties

A wide range of effects that can influence the measurement of the effective $B_s^0 \rightarrow K^+K^-$ lifetime has been evaluated. The individual contributions to the systematic uncertainties are described below and their estimated values are summarised in Table 1.

The key principle of this analysis is that the trigger and event selection do not bias the decay time distribution of the selected $B_s^0 \rightarrow K^+K^-$ candidates other than in a trivial way through a minimum decay time requirement. This has been tested extensively using simulated events at each stage of the selection process to demonstrate that no step introduces a time-dependent acceptance. Fig. 2 shows the efficiency of the full trigger and event selection as a function of decay time for simulated $B_s^0 \rightarrow K^+K^-$ candidates. The graph is fitted with a first order polynomial with a gradient of $-0.09 \pm 0.30 \text{ ns}^{-1}$ consistent with a uniform acceptance. Possible discrepancies between simulated and real events are considered by comparing the distributions of variables used by the neural networks and good agreement is observed. The available quantity of simulated events limits any non-zero gradient in the acceptance to within 0.30 ns^{-1} . This limit is used to evaluate the shift in the

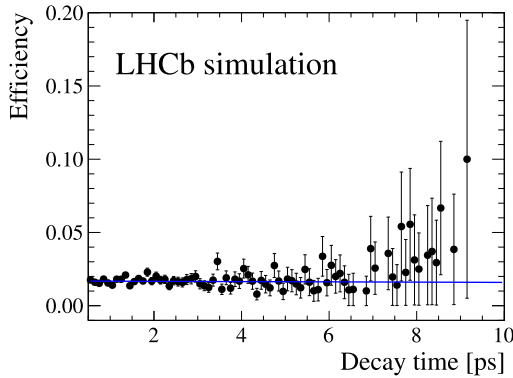


Fig. 2. Combined efficiency of LHCb trigger, selection neural networks and particle identification requirements as a function of decay time for simulated $B_s^0 \rightarrow K^+K^-$ signal candidates.

measured effective lifetime due to the presence of a linear acceptance and a negligible deviation is observed and is not considered any further.

Studies using simulated events have demonstrated that the efficiency with which tracks are reconstructed decreases as the impact parameter of the track with respect to the beam line (IP_z) increases. This introduces a decay time acceptance that may bias the measured lifetime. Such a systematic bias has been evaluated using a combination of data and simulated events. First, the effective lifetime of simulated $B_s^0 \rightarrow K^+K^-$ signal candidates is found after reconstruction to deviate by 5 fs from the generated value. Second, the tracking efficiency is parametrised as a function of IP_z using simulated events. The calculated efficiency is then applied as a weight to events in data according to their IP_z values and the effective lifetime is evaluated. This produces a deviation of 4 fs with respect to the unweighted events. The larger of these two shifts is taken as the systematic uncertainty introduced by the reconstruction acceptance.

The invariant mass distribution of $B_s^0 \rightarrow K^+K^-$ signal candidates is modelled using a Gaussian function. Potential systematic effects due to this parametrisation are evaluated by using the sum of two Gaussian functions to model additional resolution effects and separately a Crystal Ball function [21] to model final state radiation. Additionally the background parametrisation is checked by replacing the first order Chebychev polynomial with an exponential function. All these changes shift the measured lifetime by approximately 1 fs which is taken as the systematic uncertainty.

The decay time distribution is fitted with an exponential function convolved with a Gaussian function to model detector resolution, where the resolution is fixed to the value obtained from simulated events. As a cross-check, the fit is performed with the resolution parameter allowed to vary and also using a simple exponential function without attempting to model detector resolution. No deviation from the default measurement of the effective lifetime is observed in either case.

The effective $B_s^0 \rightarrow K^+K^-$ lifetime measurement has been evaluated using an alternative method which makes a simultaneous fit to the invariant mass and decay time distributions. This approach requires a parametrisation of the background decay time distribution since the *sPlot* technique is not used. Both methods give equivalent numerical results.

A wide range of different approaches to the training of the neural network have been tested, as well as the influence of different alignment and calibration settings and the number of simultaneous primary interactions in the detector. All results obtained in these checks are consistent with the result of the default analysis.

The measured decay times of B meson candidates are determined from the distance between the primary interaction and the secondary decay vertex in the silicon vertex detector. A systematic bias may therefore be introduced due to uncertainty on the LHCb length scale. This effect is estimated by considering the uncertainty on the length scale from the mechanical survey, thermal expansion and the current alignment precision. The uncertainty on the length of the detector along the beam-line is determined to be the dominant effect and a corresponding systematic uncertainty is assigned.

The effective lifetime is obtained by fitting a single exponential function to the distribution given by Eq. (1). However, the requirement that the decay time be greater than 0.5 ps diminishes the Γ_L component relative to the Γ_H component in the decay time distribution. This effect has been evaluated using simulated events and a deviation of 1 fs from the result of a fit to the full decay time range is observed.

If the production rates, R , of B_s^0 and \bar{B}_s^0 mesons are not equal then an additional oscillatory term is introduced into the decay time distribution given in Eq. (1), proportional to the production asymmetry $A_P \equiv [R(\bar{B}_s^0) - R(B_s^0)]/[R(\bar{B}_s^0) + R(B_s^0)]$. This term may alter the measured effective lifetime. Since the B_s^0 meson shares no valence quarks with the proton $A_P(B_s^0)$ at LHCb is expected to be small. Making the conservative assumption that the $|A_P(B_s^0)| = |A_P(\bar{B}_s^0)| = 0.01$ [22] we find a shift from the expected value of the effective lifetime of 2 fs using simulated events. This value is assigned as the systematic uncertainty.

6. Conclusions

Two-body charmless B decays offer a rich phenomenology to explore the phase structure of the CKM matrix and to search for manifestations of physics beyond the SM. The effective lifetime of the decay $B_s^0 \rightarrow K^+K^-$ is of considerable theoretical interest as it is sensitive to new particles entering at loop level. A measurement of this quantity is made possible by the excellent particle identification capabilities of the LHCb experiment.

The effective lifetime of the decay mode $B_s^0 \rightarrow K^+K^-$ is measured using 1.0 fb^{-1} of data recorded by the LHCb detector in 2011. A key element of this analysis is that the trigger and event selection selects B mesons without biasing the decay time distribution. This is achieved using a series of neural networks. Although this dedicated trigger has a lower efficiency compared to the one used in the previous LHCb measurement [6], it has the advantage of avoiding systematic uncertainties related to the depletion of candidates at low decay times and provides an independent approach to measuring the $B_s^0 \rightarrow K^+K^-$ effective lifetime. It is measured as

$$\tau_{KK} = 1.455 \pm 0.046 \text{ (stat.)} \pm 0.006 \text{ (syst.) ps,}$$

in good agreement with the SM prediction of 1.40 ± 0.02 ps and with the measurement on data recorded by LHCb in 2010 of $1.440 \pm 0.096 \text{ (stat.)} \pm 0.008 \text{ (syst.)} \pm 0.003 \text{ (mod.) ps}$ [6].

Acknowledgements

We express our gratitude to our colleagues in the CERN accelerator departments for the excellent performance of the LHC. We thank the technical and administrative staff at CERN and at the LHCb institutes, and acknowledge support from the National Agencies: CAPES, CNPq, FAPERJ and FINEP (Brazil); CERN; NSFC (China); CNRS/IN2P3 (France); BMBF, DFG, HGF and MPG (Germany); SFI (Ireland); INFN (Italy); FOM and NWO (The Netherlands); SCSR

(Poland); ANCS (Romania); MinES of Russia and Rosatom (Russia); MICINN, XuntaGal and GENCAT (Spain); SNSF and SER (Switzerland); NAS Ukraine (Ukraine); STFC (United Kingdom); NSF (USA). We also acknowledge the support received from the ERC under FP7 and the Region Auvergne.

Open access

This article is published Open Access at [sciencedirect.com](http://www.sciencedirect.com). It is distributed under the terms of the Creative Commons Attribution License 3.0, which permits unrestricted use, distribution, and reproduction in any medium, provided the original authors and source are credited.

References

- [1] Y. Grossman, Phys. Lett. B 380 (1996) 99.
- [2] A. Lenz, U. Nierste, JHEP 0706 (2007) 72.
- [3] R. Fleischer, R. Kneegjens, Eur. Phys. J. C 71 (2011) 1532.
- [4] R. Fleischer, Eur. Phys. J. C 52 (2007) 267.

- [5] A. Abulencia, et al., Phys. Rev. Lett. 97 (2006) 211802.
- [6] R. Aaij, et al., Phys. Lett. B 707 (2012) 349.
- [7] J. Beringer, et al., Phys. Rev. D 86 (2012) 010001.
- [8] K. Hartkorn, H. Moser, Eur. Phys. J. C 8 (1999) 381.
- [9] K. de Bruyn, R. Fleischer, R. Kneegjens, P. Koppenburg, M. Merk, et al., Phys. Rev. D 86 (2012) 014027, <http://dx.doi.org/10.1103/PhysRevD.86.014027>.
- [10] D. Asner, et al., Averages of b-hadron, c-hadron, and τ -lepton properties, arXiv: 1010.1589 [hep-ex], 2010.
- [11] R. Fleischer, R. Kneegjens, Eur. Phys. J. C 71 (2011) 1789.
- [12] A.A. Alves Jr., et al., JINST 3 (2008) S08005.
- [13] T. Sjöstrand, S. Mrenna, P. Skands, JHEP 0605 (2006) 026.
- [14] I. Belyaev, et al., in: Nuclear Science Symposium Conference Record (NSS/MIC), IEEE, 2010, p. 1155.
- [15] D.J. Lange, Nucl. Instrum. Meth. A 462 (2001) 152.
- [16] S. Agostinelli, et al., Nucl. Instrum. Meth. A 506 (2003) 250.
- [17] M. Clemencic, et al., Journal of Physics: Conference Series 331 (2011).
- [18] P. Golonka, Z. Was, Eur. Phys. J. C 45 (2006) 97.
- [19] M. Feindt, U. Kerzel, Nucl. Instrum. Meth. A 559 (2006) 190.
- [20] M. Pivk, F.R. Le, Nucl. Instrum. Meth. A 555 (2005) 356.
- [21] T. Skwarnicki, A study of the radiative cascade transitions between the Upsilon-prime and Upsilon resonances, PhD thesis, Institute of Nuclear Physics, Krakow, 1986, DESY-F31-86-DESY-F31-02.
- [22] R. Aaij, et al., Phys. Rev. Lett. 108 (2012) 201601.

LHCb Collaboration

R. Aaij³⁸, C. Abellan Beteta^{33,n}, A. Adametz¹¹, B. Adeva³⁴, M. Adinolfi⁴³, C. Adrover⁶, A. Affolder⁴⁹, Z. Ajaltouni⁵, J. Albrecht³⁵, F. Alessio³⁵, M. Alexander⁴⁸, S. Ali³⁸, G. Alkhazov²⁷, P. Alvarez Cartelle³⁴, A.A. Alves Jr.²², S. Amato², Y. Amhis³⁶, J. Anderson³⁷, R.B. Appleby⁵¹, O. Aquines Gutierrez¹⁰, F. Archilli^{18,35}, A. Artamonov³², M. Artuso^{53,35}, E. Aslanides⁶, G. Auriemma^{22,m}, S. Bachmann¹¹, J.J. Back⁴⁵, V. Balagura^{28,35}, W. Baldini¹⁶, R.J. Barlow⁵¹, C. Barschel³⁵, S. Barsuk⁷, W. Barter⁴⁴, A. Bates⁴⁸, C. Bauer¹⁰, Th. Bauer³⁸, A. Bay³⁶, J. Beddow⁴⁸, I. Bediaga¹, S. Belogurov²⁸, K. Belous³², I. Belyaev²⁸, E. Ben-Haim⁸, M. Benayoun⁸, G. Bencivenni¹⁸, S. Benson⁴⁷, J. Benton⁴³, R. Bernet³⁷, M.-O. Bettler¹⁷, M. van Beuzekom³⁸, A. Bien¹¹, S. Bifani¹², T. Bird⁵¹, A. Bizzeti^{17,h}, P.M. Bjørnstad⁵¹, T. Blake³⁵, F. Blanc³⁶, C. Blanks⁵⁰, J. Blouw¹¹, S. Blusk⁵³, A. Bobrov³¹, V. Bocci²², A. Bondar³¹, N. Bondar²⁷, W. Bonivento¹⁵, S. Borghi^{48,51}, A. Borgia⁵³, T.J.V. Bowcock⁴⁹, C. Bozzi¹⁶, T. Brambach⁹, J. van den Brand³⁹, J. Bressieux³⁶, D. Brett⁵¹, M. Britsch¹⁰, T. Britton⁵³, N.H. Brook⁴³, H. Brown⁴⁹, A. Büchler-Germann³⁷, I. Burducea²⁶, A. Bursche³⁷, J. Buytaert³⁵, S. Cadeddu¹⁵, O. Callot⁷, M. Calvi^{20,j}, M. Calvo Gomez^{33,n}, A. Camboni³³, P. Campana^{18,35}, A. Carbone¹⁴, G. Carboni^{21,k}, R. Cardinale^{19,35,i}, A. Cardini¹⁵, L. Carson⁵⁰, K. Carvalho Akiba², G. Casse⁴⁹, M. Cattaneo³⁵, Ch. Cauet⁹, M. Charles⁵², Ph. Charpentier³⁵, P. Chen^{3,36}, N. Chiapolini³⁷, M. Chrzaszcz²³, K. Ciba³⁵, X. Cid Vidal³⁴, G. Ciezarek⁵⁰, P.E.L. Clarke⁴⁷, M. Clemencic³⁵, H.V. Cliff^{44,*}, J. Closier³⁵, C. Coca²⁶, V. Coco³⁸, J. Cogan⁶, E. Cogneras⁵, P. Collins³⁵, A. Comerma-Montells³³, A. Contu⁵², A. Cook⁴³, M. Coombes⁴³, G. Corti³⁵, B. Couturier³⁵, G.A. Cowan³⁶, D. Craik⁴⁵, R. Currie⁴⁷, C. D'Ambrosio³⁵, P. David⁸, P.N.Y. David³⁸, I. De Bonis⁴, K. De Bruyn³⁸, S. De Capua^{21,k}, M. De Cian³⁷, J.M. De Miranda¹, L. De Paula², P. De Simone¹⁸, D. Decamp⁴, M. Deckenhoff⁹, H. Degaudenzi^{36,35}, L. Del Buono⁸, C. Deplano¹⁵, D. Derkach^{14,35}, O. Deschamps⁵, F. Dettori³⁹, J. Dickens⁴⁴, H. Dijkstra³⁵, P. Diniz Batista¹, F. Domingo Bonal^{33,n}, S. Donleavy⁴⁹, F. Dordei¹¹, A. Dosil Suárez³⁴, D. Dossett⁴⁵, A. Dovbnya⁴⁰, F. Dupertuis³⁶, R. Dzhelyadin³², A. Dziurda²³, A. Dzyuba²⁷, S. Easo⁴⁶, U. Egede⁵⁰, V. Egorychev²⁸, S. Eidelman³¹, D. van Eijk³⁸, F. Eisele¹¹, S. Eisenhardt⁴⁷, R. Ekelhof⁹, L. Eklund⁴⁸, I. El Rifai⁵, Ch. Elsasser³⁷, D. Elsby⁴², D. Esperante Pereira³⁴, A. Falabella^{16,14,e}, C. Färber¹¹, G. Fardell⁴⁷, C. Farinelli³⁸, S. Farry¹², V. Fave³⁶, V. Fernandez Albor³⁴, M. Ferro-Luzzi³⁵, S. Filippov³⁰, C. Fitzpatrick⁴⁷, M. Fontana¹⁰, F. Fontanelli^{19,i}, R. Forty³⁵, O. Francisco², M. Frank³⁵, C. Frei³⁵, M. Frosini^{17,f}, S. Furcas²⁰, A. Gallas Torreira³⁴, D. Galli^{14,c}, M. Gandelman², P. Gandini⁵², Y. Gao³, J.-C. Garnier³⁵, J. Garofoli⁵³, J. Garra Tico⁴⁴, L. Garrido³³, D. Gascon³³, C. Gaspar³⁵, R. Gauld⁵², N. Gauvin³⁶, E. Gersabeck¹¹, M. Gersabeck³⁵, T. Gershon^{45,35}, Ph. Ghez⁴, V. Gibson⁴⁴, V.V. Gligorov³⁵, C. Göbel⁵⁴, D. Golubkov²⁸, A. Golutvin^{50,28,35}, A. Gomes², H. Gordon⁵², M. Grabalosa Gándara³³, R. Graciani Diaz³³, L.A. Granado Cardoso³⁵, E. Graugés³³, G. Graziani¹⁷, A. Grecu²⁶, E. Greening⁵², S. Gregson⁴⁴, O. Grünberg⁵⁵, B. Gui⁵³, E. Gushchin³⁰, Yu. Guz³², T. Gys³⁵, C. Hadjivasiliou⁵³, G. Haefeli³⁶, C. Haen³⁵, S.C. Haines⁴⁴, T. Hampson⁴³, S. Hansmann-Menzemer¹¹, N. Harnew⁵², S.T. Harnew⁴³, J. Harrison⁵¹, P.F. Harrison⁴⁵, T. Hartmann⁵⁵, J. He⁷, V. Heijne³⁸, K. Hennessy⁴⁹, P. Henrard⁵, J.A. Hernando Morata³⁴,

E. van Herwijnen³⁵, E. Hicks⁴⁹, M. Hoballah⁵, P. Hopchev⁴, W. Hulsbergen³⁸, P. Hunt⁵², T. Huse⁴⁹, R.S. Huston¹², D. Hutchcroft⁴⁹, D. Hynds⁴⁸, V. Iakovenko⁴¹, P. Ilten¹², J. Imong⁴³, R. Jacobsson³⁵, A. Jaeger¹¹, M. Jahjah Hussein⁵, E. Jans³⁸, F. Jansen³⁸, P. Jaton³⁶, B. Jean-Marie⁷, F. Jing³, M. John⁵², D. Johnson⁵², C.R. Jones⁴⁴, B. Jost³⁵, M. Kabbalo⁹, S. Kandybei⁴⁰, M. Karacson³⁵, T.M. Karbach⁹, J. Keaveney¹², I.R. Kenyon⁴², U. Kerzel³⁵, T. Ketel³⁹, A. Keune³⁶, B. Khanji⁶, Y.M. Kim⁴⁷, M. Knecht³⁶, O. Kochebina⁷, I. Komarov²⁹, R.F. Koopman³⁹, P. Koppenburg³⁸, M. Korolev²⁹, A. Kozlinskiy³⁸, L. Kravchuk³⁰, K. Kreplin¹¹, M. Kreps⁴⁵, G. Krocker¹¹, P. Krokovny³¹, F. Kruse⁹, K. Kruzelecki³⁵, M. Kucharczyk^{20,23,35,j}, V. Kudryavtsev³¹, T. Kvaratskheliya^{28,35}, V.N. La Thi³⁶, D. Lacarrere³⁵, G. Lafferty⁵¹, A. Lai¹⁵, D. Lambert⁴⁷, R.W. Lambert³⁹, E. Lanciotti³⁵, G. Lanfranchi¹⁸, C. Langenbruch³⁵, T. Latham⁴⁵, C. Lazzeroni⁴², R. Le Gac⁶, J. van Leerdam³⁸, J.-P. Lees⁴, R. Lefèvre⁵, A. Leflat^{29,35}, J. Lefrançois⁷, O. Leroy⁶, T. Lesiak²³, L. Li³, Y. Li³, L. Li Gioi⁵, M. Lieng⁹, M. Liles⁴⁹, R. Lindner³⁵, C. Linn¹¹, B. Liu³, G. Liu³⁵, J. von Loeben²⁰, J.H. Lopes², E. Lopez Asamar³³, N. Lopez-March³⁶, H. Lu³, J. Luisier³⁶, A. Mac Raighne⁴⁸, F. Machefert⁷, I.V. Machikhiliyan^{4,28}, F. Maciuc¹⁰, O. Maev^{27,35}, J. Magnin¹, S. Malde⁵², R.M.D. Mamunur³⁵, G. Manca^{15,d}, G. Mancinelli⁶, N. Mangiafave⁴⁴, U. Marconi¹⁴, R. Märki³⁶, J. Marks¹¹, G. Martellotti²², A. Martens⁸, L. Martin⁵², A. Martín Sánchez⁷, M. Martinelli³⁸, D. Martinez Santos³⁵, A. Massafferri¹, Z. Mathe¹², C. Matteuzzi²⁰, M. Matveev²⁷, E. Maurice⁶, B. Maynard⁵³, A. Mazurov^{16,30,35}, J. McCarthy⁴², G. McGregor⁵¹, R. McNulty¹², M. Meissner¹¹, M. Merk³⁸, J. Merkel⁹, D.A. Milanes¹³, M.-N. Minard⁴, J. Molina Rodriguez⁵⁴, S. Monteil⁵, D. Moran¹², P. Morawski²³, R. Mountain⁵³, I. Mous³⁸, F. Muheim⁴⁷, K. Müller³⁷, R. Muresan²⁶, B. Muryn²⁴, B. Muster³⁶, J. Mylroie-Smith⁴⁹, P. Naik⁴³, T. Nakada³⁶, R. Nandakumar⁴⁶, I. Nasteva¹, M. Needham⁴⁷, N. Neufeld³⁵, A.D. Nguyen³⁶, C. Nguyen-Mau^{36,o}, M. Nicol⁷, V. Niess⁵, N. Nikitin²⁹, T. Nikodem¹¹, A. Nomerotski^{52,35}, A. Novoselov³², A. Oblakowska-Mucha²⁴, V. Obraztsov³², S. Oggero³⁸, S. Ogilvy⁴⁸, O. Okhrimenko⁴¹, R. Oldeman^{15,35,d}, M. Orlandea²⁶, J.M. Otalora Goicochea², P. Owen⁵⁰, B.K. Pal⁵³, J. Palacios³⁷, A. Palano^{13,b}, M. Palutan¹⁸, J. Panman³⁵, A. Papanestis⁴⁶, M. Pappagallo⁴⁸, C. Parkes⁵¹, C.J. Parkinson⁵⁰, G. Passaleva¹⁷, G.D. Patel⁴⁹, M. Patel⁵⁰, G.N. Patrick⁴⁶, C. Patrignani^{19,i}, C. Pavel-Nicorescu²⁶, A. Pazos Alvarez³⁴, A. Pellegrino³⁸, G. Penso^{22,l}, M. Pepe Altarelli³⁵, S. Perazzini^{14,c}, D.L. Perego^{20,j}, E. Perez Trigo³⁴, A. Pérez-Calero Yzquierdo³³, P. Perret⁵, M. Perrin-Terrin⁶, G. Pessina²⁰, A. Petrolini^{19,i}, A. Phan⁵³, E. Picatoste Olloqui³³, B. Pie Valls³³, B. Pietrzyk⁴, T. Pilař⁴⁵, D. Pinci²², R. Plackett⁴⁸, S. Playfer⁴⁷, M. Plo Casasus³⁴, F. Polci⁸, G. Polok²³, A. Poluektov^{45,31}, E. Polcarpo², D. Popov¹⁰, B. Popovici²⁶, C. Potterat³³, A. Powell⁵², J. Prisciandaro³⁶, V. Pugatch⁴¹, A. Puig Navarro³³, W. Qian⁵³, J.H. Rademacker⁴³, B. Rakotomiaramanana³⁶, M.S. Rangel², I. Raniuk⁴⁰, G. Raven³⁹, S. Redford⁵², M.M. Reid⁴⁵, A.C. dos Reis¹, S. Ricciardi⁴⁶, A. Richards⁵⁰, K. Rinnert⁴⁹, D.A. Roa Romero⁵, P. Robbe⁷, E. Rodrigues^{48,51}, F. Rodrigues², P. Rodriguez Perez³⁴, G.J. Rogers⁴⁴, S. Roiser³⁵, V. Romanovsky³², M. Rosello^{33,n}, J. Rouvinet³⁶, T. Ruf³⁵, H. Ruiz³³, G. Sabatino^{21,k}, J.J. Saborido Silva³⁴, N. Sagidova²⁷, P. Sail⁴⁸, B. Saitta^{15,d}, C. Salzmann³⁷, B. Sanmartin Sedes³⁴, M. Sannino^{19,i}, R. Santacesaria²², C. Santamarina Rios³⁴, R. Santinelli³⁵, E. Santovetti^{21,k}, M. Sapunov⁶, A. Sarti^{18,l}, C. Satriano^{22,m}, A. Satta²¹, M. Savrie^{16,e}, D. Savrina²⁸, P. Schaack⁵⁰, M. Schiller³⁹, H. Schindler³⁵, S. Schleich⁹, M. Schlupp⁹, M. Schmelling¹⁰, B. Schmidt³⁵, O. Schneider³⁶, A. Schopper³⁵, M.-H. Schune⁷, R. Schwemmer³⁵, B. Sciascia¹⁸, A. Sciubba^{18,l}, M. Seco³⁴, A. Semennikov²⁸, K. Senderowska²⁴, I. Sepp⁵⁰, N. Serra³⁷, J. Serrano⁶, P. Seyfert¹¹, M. Shapkin³², I. Shapoval^{40,35}, P. Shatalov²⁸, Y. Shcheglov²⁷, T. Shears⁴⁹, L. Shekhtman³¹, O. Shevchenko⁴⁰, V. Shevchenko²⁸, A. Shires⁵⁰, R. Silva Coutinho⁴⁵, T. Skwarnicki⁵³, N.A. Smith⁴⁹, E. Smith^{52,46}, M. Smith⁵¹, K. Sobczak⁵, F.J.P. Soler⁴⁸, A. Solomin⁴³, F. Soomro^{18,35}, D. Souza⁴³, B. Souza De Paula², B. Spaan⁹, A. Sparkes⁴⁷, P. Spradlin⁴⁸, F. Stagni³⁵, S. Stahl¹¹, O. Steinkamp³⁷, S. Stoica²⁶, S. Stone^{53,35}, B. Storaci³⁸, M. Straticiu²⁶, U. Straumann³⁷, V.K. Subbiah³⁵, S. Swientek⁹, M. Szczekowski²⁵, P. Szczypka³⁶, T. Szumlak²⁴, S. T'Jampens⁴, M. Teklishyn⁷, E. Teodorescu²⁶, F. Teubert³⁵, C. Thomas⁵², E. Thomas³⁵, J. van Tilburg¹¹, V. Tisserand⁴, M. Tobin³⁷, S. Tolk³⁹, S. Topp-Joergensen⁵², N. Torr⁵², E. Tournefier^{4,50}, S. Tourneur³⁶, M.T. Tran³⁶, A. Tsaregorodtsev⁶, N. Tuning³⁸, M. Ubeda Garcia³⁵, A. Ukleja²⁵, U. Uwer¹¹, V. Vagnoni¹⁴, G. Valenti¹⁴, R. Vazquez Gomez³³, P. Vazquez Regueiro³⁴, S. Vecchi¹⁶, J.J. Velthuis⁴³, M. Veltri^{17,g}, M. Vesterinen³⁵, B. Viaud⁷, I. Videau⁷, D. Vieira², X. Vilasis-Cardona^{33,n}, J. Visniakov³⁴, A. Vollhardt³⁷, D. Volyanskyy¹⁰, D. Voong⁴³, A. Vorobyev²⁷, V. Vorobyev³¹, C. Voß⁵⁵, H. Voss¹⁰, R. Waldi⁵⁵,

R. Wallace¹², S. Wandernoth¹¹, J. Wang⁵³, D.R. Ward⁴⁴, N.K. Watson⁴², A.D. Webber⁵¹, D. Websdale⁵⁰, M. Whitehead⁴⁵, J. Wicht³⁵, D. Wiedner¹¹, L. Wiggers³⁸, G. Wilkinson⁵², M.P. Williams^{45,46}, M. Williams⁵⁰, F.F. Wilson⁴⁶, J. Wishahi⁹, M. Witek²³, W. Witzeling³⁵, S.A. Wotton⁴⁴, S. Wright⁴⁴, S. Wu³, K. Wyllie³⁵, Y. Xie⁴⁷, F. Xing⁵², Z. Xing⁵³, Z. Yang³, R. Young⁴⁷, X. Yuan³, O. Yushchenko³², M. Zangoli¹⁴, M. Zavertyaev^{10,a}, F. Zhang³, L. Zhang⁵³, W.C. Zhang¹², Y. Zhang³, A. Zhelezov¹¹, L. Zhong³, A. Zvyagin³⁵

¹ Centro Brasileiro de Pesquisas Físicas (CBPF), Rio de Janeiro, Brazil

² Universidade Federal do Rio de Janeiro (UFRJ), Rio de Janeiro, Brazil

³ Center for High Energy Physics, Tsinghua University, Beijing, China

⁴ LAPP, Université de Savoie, CNRS/IN2P3, Annecy-Le-Vieux, France

⁵ Clermont Université, Université Blaise Pascal, CNRS/IN2P3, LPC, Clermont-Ferrand, France

⁶ CPPM, Aix-Marseille Université, CNRS/IN2P3, Marseille, France

⁷ LAL, Université Paris-Sud, CNRS/IN2P3, Orsay, France

⁸ LPNHE, Université Pierre et Marie Curie, Université Paris Diderot, CNRS/IN2P3, Paris, France

⁹ Fakultät Physik, Technische Universität Dortmund, Dortmund, Germany

¹⁰ Max-Planck-Institut für Kernphysik (MPIK), Heidelberg, Germany

¹¹ Physikalisches Institut, Ruprecht-Karls-Universität Heidelberg, Heidelberg, Germany

¹² School of Physics, University College Dublin, Dublin, Ireland

¹³ Sezione INFN di Bari, Bari, Italy

¹⁴ Sezione INFN di Bologna, Bologna, Italy

¹⁵ Sezione INFN di Cagliari, Cagliari, Italy

¹⁶ Sezione INFN di Ferrara, Ferrara, Italy

¹⁷ Sezione INFN di Firenze, Firenze, Italy

¹⁸ Laboratori Nazionali dell'INFN di Frascati, Frascati, Italy

¹⁹ Sezione INFN di Genova, Genova, Italy

²⁰ Sezione INFN di Milano Bicocca, Milano, Italy

²¹ Sezione INFN di Roma Tor Vergata, Roma, Italy

²² Sezione INFN di Roma La Sapienza, Roma, Italy

²³ Henryk Niewodniczanski Institute of Nuclear Physics Polish Academy of Sciences, Kraków, Poland

²⁴ AGH University of Science and Technology, Kraków, Poland

²⁵ Soltan Institute for Nuclear Studies, Warsaw, Poland

²⁶ Horia Hulubei National Institute of Physics and Nuclear Engineering, Bucharest-Magurele, Romania

²⁷ Petersburg Nuclear Physics Institute (PNPI), Gatchina, Russia

²⁸ Institute of Theoretical and Experimental Physics (ITEP), Moscow, Russia

²⁹ Institute of Nuclear Physics, Moscow State University (SINP MSU), Moscow, Russia

³⁰ Institute for Nuclear Research of the Russian Academy of Sciences (INR RAN), Moscow, Russia

³¹ Budker Institute of Nuclear Physics (SB RAS) and Novosibirsk State University, Novosibirsk, Russia

³² Institute for High Energy Physics (IHEP), Protvino, Russia

³³ Universitat de Barcelona, Barcelona, Spain

³⁴ Universidad de Santiago de Compostela, Santiago de Compostela, Spain

³⁵ European Organization for Nuclear Research (CERN), Geneva, Switzerland

³⁶ Ecole Polytechnique Fédérale de Lausanne (EPFL), Lausanne, Switzerland

³⁷ Physik-Institut, Universität Zürich, Zürich, Switzerland

³⁸ Nikhef National Institute for Subatomic Physics, Amsterdam, The Netherlands

³⁹ Nikhef National Institute for Subatomic Physics and VU University Amsterdam, Amsterdam, The Netherlands

⁴⁰ NSC Kharkiv Institute of Physics and Technology (NSC KIPT), Kharkiv, Ukraine

⁴¹ Institute for Nuclear Research of the National Academy of Sciences (KINR), Kyiv, Ukraine

⁴² University of Birmingham, Birmingham, United Kingdom

⁴³ H.H. Wills Physics Laboratory, University of Bristol, Bristol, United Kingdom

⁴⁴ Cavendish Laboratory, University of Cambridge, Cambridge, United Kingdom

⁴⁵ Department of Physics, University of Warwick, Coventry, United Kingdom

⁴⁶ STFC Rutherford Appleton Laboratory, Didcot, United Kingdom

⁴⁷ School of Physics and Astronomy, University of Edinburgh, Edinburgh, United Kingdom

⁴⁸ School of Physics and Astronomy, University of Glasgow, Glasgow, United Kingdom

⁴⁹ Oliver Lodge Laboratory, University of Liverpool, Liverpool, United Kingdom

⁵⁰ Imperial College London, London, United Kingdom

⁵¹ School of Physics and Astronomy, University of Manchester, Manchester, United Kingdom

⁵² Department of Physics, University of Oxford, Oxford, United Kingdom

⁵³ Syracuse University, Syracuse, NY, United States

⁵⁴ Pontifícia Universidade Católica do Rio de Janeiro (PUC-Rio), Rio de Janeiro, Brazil^P

⁵⁵ Institut für Physik, Universität Rostock, Rostock, Germany^Q

* Corresponding author.

E-mail address: cliff@hep.phy.cam.ac.uk (H.V. Cliff).

^a P.N. Lebedev Physical Institute, Russian Academy of Science (LPI RAS), Moscow, Russia.

^b Università di Bari, Bari, Italy.

^c Università di Bologna, Bologna, Italy.

^d Università di Cagliari, Cagliari, Italy.

^e Università di Ferrara, Ferrara, Italy.

^f Università di Firenze, Firenze, Italy.

^g Università di Urbino, Urbino, Italy.

^h Università di Modena e Reggio Emilia, Modena, Italy.

ⁱ Università di Genova, Genova, Italy.

^j Università di Milano Bicocca, Milano, Italy.

^k Università di Roma Tor Vergata, Roma, Italy.

^l Università di Roma La Sapienza, Roma, Italy.

^m Università della Basilicata, Potenza, Italy.

ⁿ LIFAELS, La Salle, Universitat Ramon Llull, Barcelona, Spain.

^o Hanoi University of Science, Hanoi, Viet Nam.

^p Associated to: Universidade Federal do Rio de Janeiro (UFRJ), Rio de Janeiro, Brazil.

^q Associated to: Physikalisches Institut, Ruprecht-Karls-Universität Heidelberg, Heidelberg, Germany.